Eur. Phys. J. B **35**, 517–524 (2003)
DOI: 10.1140/epjb/e2003-00305-2

THE EUROPEAN PHYSICAL JOURNAL B

Ag deposited onto the (100) surface in silicon studied by Density Functional Theory and Classical Molecular Dynamics

A.M. Mazzone[a]

C.N.R. - Istituto IMM-Sezione di Bologna-Via Gobetti 101, 40129 Bologna, Italy

Received 5 May 2003 / Received in final form 21 July 2003
Published online 24 October 2003 – © EDP Sciences, Società Italiana di Fisica, Springer-Verlag 2003

Abstract. Numerous theoretical studies have been dedicated to Ag deposited on Si(111) and the properties of this system are now well assessed. On the contrary, the interface Ag/Si(100) is more elusive and several problems of this system have not been satisfactorily solved yet. In this work the Density Functional theory with GGA corrections and Molecular Dynamics simulations with classical interatomic potentials have been applied to the evaluation of adsorption of Ag on Si(100). Small clusters representing a fragment of the exposed surface are used in GGA calculations to study the chemistry of Ag/Si bonds in dependence of the shape, bulk-terminated or dimerized, of the Si(100) surface. Isothermal molecular dynamics simulations describe the motions of the diffusing adatoms in a temperature range from T=10 to 1000 K. The results indicate that the Ag atoms are adsorbed in a cave site among surface atoms, a feature consistent with experimental observations. Furthermore it is shown that, though there are no contradiction between the two methods, the difference between the stationary GGA and the dynamical MD evaluation is noticeable. This result has both practical and conceptual relevance.

PACS. 71.15.Mb Density functional theory, local density approximation, gradient and other corrections – 71.15.Pd Molecular dynamics calculations (Car-Parrinello) and other numerical simulations – 81.10.Aj Theory and models of crystal growth; physics of crystal growth, crystal morphology and orientation

1 Introduction

There is currently a considerable interest for deposition of thin metallic films on a semiconductor substrate. In fact, the film electronic properties, such as Schottky barrier height and electron transport in quantum devices, are influenced by the atomic details of the interface structure.

In this field a noticeable example is offered by silver deposited on silicon. Most metals interact strongly with Si and form silicides. However there is no silicide formation at the Ag/Si interface and the interface between the two elements is considered as atomically sharp. Therefore a change from semiconductor to metallic behaviour is bound to occur across only one atomic layer. Furthermore Ag is a monovalent metal and forms close-packed structures to maximize the sharing of the conduction electrons. In contrast, Si has four valence electrons whose orbital structure favors tetrahedral directional bonding. Due to these differences and to the scarce reactivity between the two elements, the adsorption of Ag on Si represents a problem of considerable complexity. The investigation on Ag deposited on Si(111) has been very intensive and for this system the questions concerning the way Ag bonds to the silicon surface have been treated theoretically in great detail using quantum mechanical methods (see [1–7] and references therein). On the contrary, the absence of any reported ordered phase has hindered extensive studies on Ag/Si(100) for a long time. The discovery of a few of such phases has revived the interest for this system and many structural characterization are now available [8–18]. However the number of theoretical studies is scanty (only [19], to the best of our knowledge) and several properties, such as the bonding between Ag and Si, the adsorption sites energetically preferred and the structure of the initial Ag layer, deserve further investigation.

The purpose of this work is the study of structural and electronic properties of Ag/Si(100) at submonolayer coverage. Preferred adsorption sites and binding energies are obtained from DFT calculation using the Generalized Gradient Approximation and a cluster model of the surface. An isothermal molecular dynamics simulation method accounts for the kinetics aspects of deposition and describes the effects of the motions of Ag atoms. According to GGA calculations, a valley site between the dimer rows is the energetically preferred adsorption site. However an even modest temperature rise leads to perceptible atomic motions and to considerable out-diffusion from the equilibrium adsorption configurations.

[a] e-mail: mazzone@bo.cnr.it

2 The simulation methods

A fundamental issue in adsorption studies is the structure of the exposed surface. This problem is of particular importance for Si(100) as this surface reconstructs strongly by the formation of dimers. However a proper annealing treatment is required to obtain dimerization and even after this treatment the surface structure is highly defective. In addition, it is known that several species of deposited atoms restore the bulk termination and this action has also been attributed to Ag deposited either on Si(111) [2] or on Si(100) [16]. Eventually, this effect complicates the interpretation of experiments as it becomes difficult to distinguish between the deposited Ag and the surface silicon atoms, the location of the latter ones being uncertain. It is therefore important to understand the effects produced by the structure of the exposed surface. To this purpose, the model (100) surface used in GGA and MD calculations has both a dimerized structure and the one with the atoms in their regular bulk locations (these structures are indicated below as Dimerized Surface (DS) and Bulk-terminated Surface (BS), respectively). A lattice view of the dimerized surface is presented in Figure 1a whereas a plane view of both DS and BS is reported in Figure 1b.

Preferred adsorption sites and binding energies have been obtained from GGA calculations using clusters of size n in the range 10–50 (clusters in a similar range of sizes have been also adopted in [4,5,19]). The clusters represent a small fragment of the exposed surface to which an Ag atom is added. A three-dimensional impression of the cluster structure is offered by Figure 1a whereas a precise indication is given in Figure 1c. This figure shows clusters containing only dimers (top panel) and dimers and subsurface atoms (bottom panel). In all cases the cluster structure is symmetric and contains the lines needed for the mapping of the adsorption energy (marked by the dotted lines). The size is increased by increasing the number of dimers and of subsurface atoms (larger clusters with second layer atoms have been omitted for the sake of clarity in the presentation). The clusters used for BS have the same structural model as the ones used for DS. However the dimers are replaced by atoms in normal lattice locations. In both cases the peripheral dangling bonds are compensated with hydrogen atoms which occupy sites with the silicon tetrahedral coordination but with a reduced interatomic distance approximately equal to 1.5 Å (in Fig. 1a the locations of H atoms are marked by the smaller circles. However, for the sake of clarity, these atoms are at the normal distance of silicon atoms).

The study of the relaxation of the clusters, performed prior to adsorption calculations, showed properties consistent with known features of Si(100). In fact, for dimers and subsurface atoms the average interatomic distance is 2.45 and 2.32 Å, respectively, and a dimer formation energy in the range 1.9 eV/atom was obtained from the comparison of the energy of DS and BS clusters.

Two common parameters used in surface studies are the binding and the adsorption energy, E_b and E_a, respectively, and also in this study the two energies are used as indicators of the quality of bonding. In the following E_b

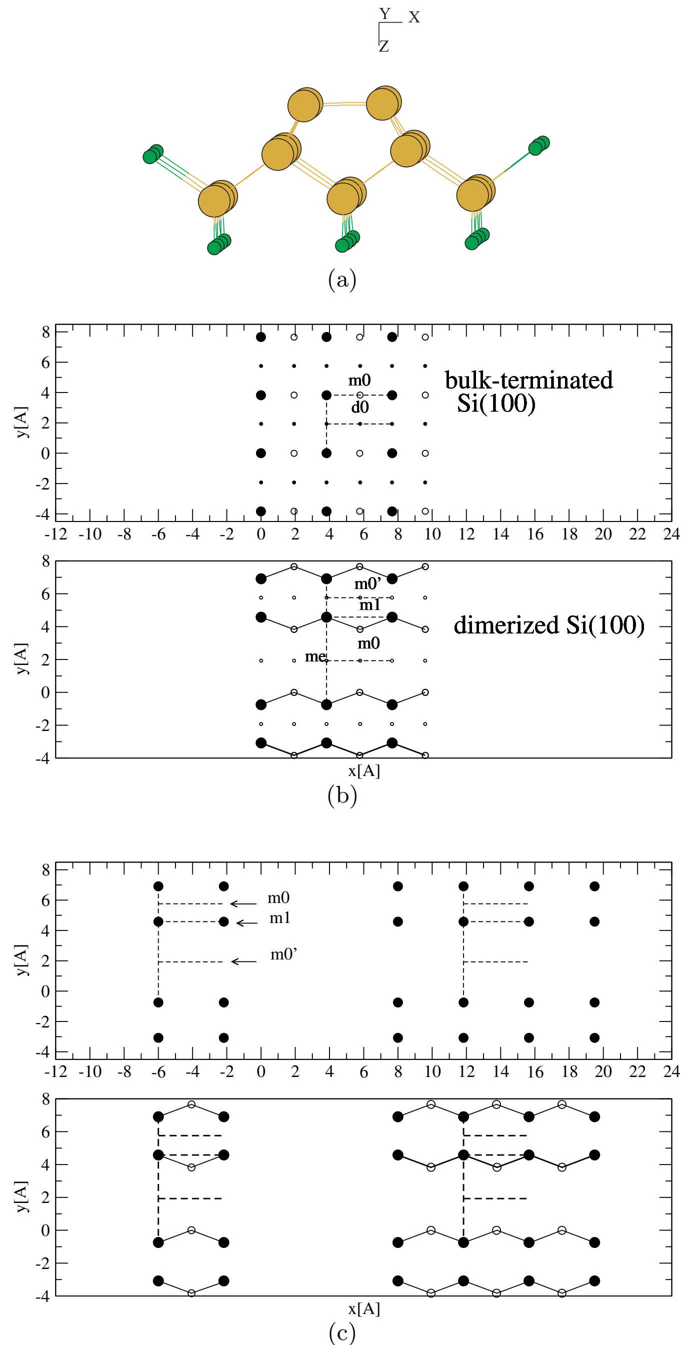

Fig. 1. (a) Structure of the cluster Si_{19} representing the dimerized Si(100) surface. Large and small circles mark silicon and hydrogen atoms, respectively. (b) Plane view of the bulk-terminated (top) and of the dimerized Si(100) surface (bottom). Surface atoms are marked by dark circles. Second- and third-layer atoms are marked by empty circles of decreasing size. The dotted lines have been used to map E_b in DeFT calculations. The lettering m marks the E_b minima. The figure also shows the x,y coordinate axis used in DeFT and MD calculations. (c) Structure of the clusters used in adsorption. Top: clusters of size 8 and 16 formed by dimers. Bottom: clusters of size 10 and 26 formed by dimers and subsurface atoms. The dotted lines show the locations of the deposited Ag and the arrows indicate to which minimum the line refers.

is evaluated from the difference between the total energy $E_t(\mathrm{Si}_n\mathrm{Ag})$ of the $\mathrm{Si}_n\mathrm{Ag}$ cluster and the one of an ensemble of free atoms of the same size and composition. The expression of E_a is

$$E_a = E_t(\mathrm{Si}_n\mathrm{Ag}) - E_t(\mathrm{Si}_n) - E_{\mathrm{Ag}},$$

where $E_t(\mathrm{Si}_n)$ and E_{Ag} indicate the energy of the clean cluster and of the free Ag atom, respectively. For both E_b and E_a a negative value indicates binding and therefore the corresponding lattice location is a possible adsorption site.

A map of these sites has been constructed by displacing Ag along the dotted lines shown in Figure 1b, c (in these figures the coordinate axes used in GGA and MD calculations are also reported). For each of the selected locations the cluster is relaxed to an energy minimum by allowing the displacement of dimers and second layers atoms. The plots in Figure 1c show that, while for $n \leq$ the potential energy sensed by the deposited atom accounts only for nearest dimers and subsurface atoms, the action of distant dimers and subsurface atoms is included at the larger sizes.

For the evaluation of the clusters electronic structure the package DeFT [20] has been used. DeFT, which belongs to the second generation of Density Functional calculations, contains the gradient-corrected Vosko-Wilk-Nusair functional and the Becke-Perdew correlation potential (this formulation is generally indicated as GGA). The electronic structure of Ag and Si is $5s5p4d$ and $3s3p$, respectively, these orbitals being represented by the DeFT default double-ζ functions.

In MD simulations, according to the method adopted in similar studies [21,22], the structure used to represent the substrate is a silicon crystal with an approximately cubic shape. The exposed (100) surface has a linear dimension in the range 30 Å and its structure is either DS or BS. Ag atoms with a selected direction of motion and energy E are deposited on this surface. To save computer time and to improve statistics several Ag atoms are deposited simultaneously and their trajectories are calculated in parallel. The resulting Ag coverage is around 0.06 and the deposition conditions can be regarded as representative of the dilute limit of the adsorbate concentration.

The evolution of the system is described using the Andersen isothermal Molecular Dynamics. This method allows to maintain a system, subject to normal interatomic forces, to the wanted temperature T by the continuous removal of the excess kinetic energy via stochastic collisions. The Oh-Johnson potential and the Tersoff potential [23,24] are used for Ag-Ag and Si-Si interactions, respectively. However, due to the dilute concentration of the adsorbate, the Ag atoms interact almost exclusively with the silicon substrate and the Ag-Si potential represents a pivotal quantity in these simulations. This potential is obtained fitting the E_b vs. R function obtained from DeFT with a simple Morse potential and the quality of this fitting is illustrated in the following paragraph.

To describe the dynamics of the atomic motions four parameters, i.e. $\langle d\rangle$, $\langle d_x^2\rangle$, $\langle d_y^2\rangle$ and $\langle d_z^2\rangle$, have been adopted. $\langle d\rangle$ is an average displacement and is evaluated from the modulus of the displacement vector from the initial location. The $\langle d^2\rangle$ coefficients represent the squared projections of $\langle d\rangle$ along x, y and z.

3 DeFT calculations of Ag adsorption on Si(100). Geometries and electronic structure

An useful introduction to the calculations reported in this section is offered by the known properties of Ag/Si(111) and Ag/Si(100). The structure of the Si(111) surface consists of trimers with atoms at the same height with a distance equal to 3.83 Å. Experiments on Ag deposition show that at temperatures between 400 and 500 °C, starting from the clean surface up to a monolayer coverage, a triangular $\sqrt{3}\times\sqrt{3}$ structure is formed. This structure changes into a linear 3×1 structure during desorption at 700 °C for coverages from 1 down to 2/3. The interpretation of these results has been controversial. It has been proposed that the possible adsorption site for the deposited Ag adatom is (*i*) above a silicon atom on the dangling orbital axis, (*ii*) above the barycenter of an equilateral triangle constituted by three adjacent Si atoms or also (*iii*) slightly embedded below the outermost silicon layer. From ab initio calculations and experiments it is now well assessed that the 3×1 pattern arises from linear chains of Ag atoms on top of silicon (position (*i*)) while the $\sqrt{3}\times\sqrt{3}$ pattern is due to Ag absorbed on the threefold hollow site (position (*ii*)). In both cases the Ag-Si distance is in the range 2.6 Å and in (*ii*) the height z of Ag above the surface is 1.48 Å [1,5].

For Si(100) it is generally agreed that Ag grows on this surface in the Stranski-Krastanov mode, though the structure of the wetting layer and of the islands above it are controversial. Also the absence of any reported ordered phase during submonolayer growth has hindered extensive investigations on this system for a long time. However the discovery of local, or long-range, patterns (i.e. 2×1, 2×2, 2×3 and c(4×2), c(6×2)) has revived a wide interest for the microscopic structure of Ag/Si(100). According to these studies (already quoted in the Introduction) the film grown at room temperature has no long-range order and only a quasi 2×2 periodicity, expanding at 2×1, is observed. The other patterns appear at temperatures above 80 °C [18]. The structure of the exposed surface is critical and determines the growth of different types of interfaces. In [9] STM studies of submonolayer deposition indicate that the bonding site of the Ag atom is between two neighboring dimer rows. In [13] it is shown that this is consistent with 2×2 and c(4×2), the formation of the one or the other phase being attributable to the Ag-induced dimer buckling. On the contrary, for 2×3 different models based on the coverage 2/3 and (1/3,1/2) have been proposed. In [16] it is shown that surface states related to dimers disappear by the formation of the coverage (1/3,1/2) which therefore reinstalls the BS structure. This also applies to c(6×2) [17].

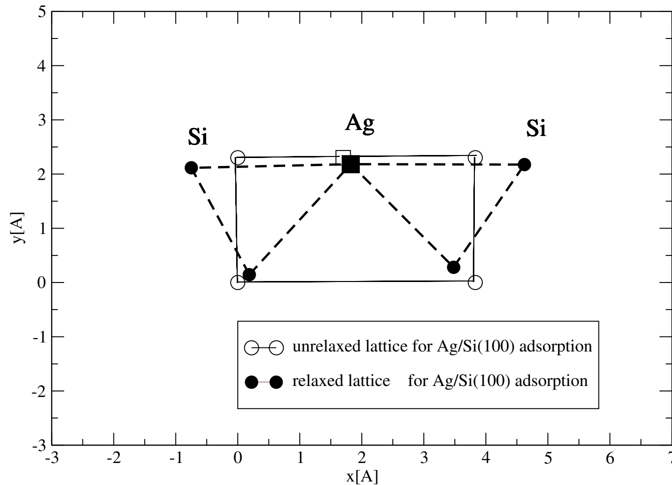

Fig. 2. The figure refers to a model calculation and shows a couple of dimers with an Ag atom embedded among them. The figure shows the initial lattice and the lattice at the end of a relaxation carried out under the constraint of minimal energy.

For Ag/Si(111) DFT and HF calculations coupled with a cluster model of the exposed surface lead to a binding and an adsorption energy both in the range 3 eV [2,5]. However also a smaller value, around 1 eV, has been obtained with calculations using superposition of the atomic spheres [4]. These divergences underline the sensitivity of adsorption to the details of the evaluation. For Ag/Si(100) a binding energy in the range 1 eV is reported in [19] using atom charge superposition. However optical adsorption measurements suggest an E_a value in the range 2.3 eV [11] and a broader range of binding energies, from 1.2 to 3.8 eV, is obtained from XPD [17].

Adsorption properties of Ag/Si(100) are illustrated in Figures 2 and 3. The first figure presents a simple sketch of the lattice relaxation upon adsorption. The second one describes the functional dependence of the binding energy E_b on the distance R between Ag and the nearest atomic location.

The calculation reported in Figure 2 refers to a model structure formed by only two dimers aligned along y (the compensating hydrogens have been omitted) and has been chosen to illustrate features common to all sites reported below in Figure 3. The calculation shows a stressed lattice under dilatation. However both the symmetry and planarity of the original structure are preserved and the adsorbed geometry is essentially defined by the Ag-Si distance. Therefore the potential energy sensed by the deposited adatom is fully characterized by the E_b vs. R relationship reported in Figure 3.

Noticeable features of the plots in Figure 3 are a broad minimum and some scattering of the data points. This last effect has two sources. First, there are fluctuations arising from different lattice locations whose distance R from Ag is, however, equal. This leads to changes in the values of E_b for both BS and DS in the range 5–10% with some maximum values around 30–70%. These large changes, however, have no effects on adsorption as they occur only at small R where E_b is positive. Second, some fluctuations are due to the fact that results obtained from clusters of different size have been projected onto the same curve. Generally, the increase of the cluster size n leads to a change of the integrated value $\int E_b dR$ in a range 2–3% with some fluctuations of E_b around 4%. This sets size-effects errors in the range of a few percents. Furthermore n has no effect on the location of the minima. As reported in the following, the differences between the E_b values at the most stable adsorption sites are in the range 10–16% and are therefore clearly distinguishable from the size-effects described above.

From Figure 3 it is seen that for both DS and BS E_b has a broad minimum at R between 2 and 3.5 Å. This indicates that several adsorption sites are possible. The locations of the deepest minima are reported in Figure 1b where they are marked by the lettering m. On the bulk-terminated surface the absolute minimum m_0 is in a bridge-site between two atomic rows at a height $z = 1.5$ Å above the surface. The corresponding E_b and R values are -2.68 eV/atom and 2.42 Å, respectively. On the dimerized surface (Fig. 1b) three regions of adsorption, i.e. m'_0, m_1 and m_0, have been found. They have approximately the same x coordinate. However m'_0 and m_1 are between two dimer rows in a pedestal and side-bridge location, respectively, while m_0 is in a valley location in the trench between dimers. The deepest minimum is m_0 whose E_b and R values are -4.23 eV/atom and 2.58 Å, respectively. The corresponding values for m'_0 and m_1 are -3.94 eV/atom and 2.20 Å and -3.65 eV and 2.30 Å, respectively.

The mapping of the adsorption energy closely follows the one of E_b. In fact the adsorption energy is at its minimum in DS (the E_a value in m_0 is -3.5 eV) and perceptibly larger in BS (-2.5 eV). For the sake of brevity a detailed account of these values has been omitted.

The important aspects of these calculations are three. First, Ag adsorption has obviously the same physical origin on Si(111) and Si(100) and in both cases bonding arises from mixing and hybridization of the dangling orbitals of the surface silicon atoms with the ones of the adsorbed Ag. Therefore qualitatively similar results are expected for the two systems. In fact, in Si(100) the adsorption site is a hollow site, which is also a feature of the $\sqrt{3} \times \sqrt{3}$ pattern in Si(111). Furthermore from Figure 2 it is seen that the relaxed lattice is formed by equilateral triangles which is also reminiscent of $\sqrt{3} \times \sqrt{3}$. Also the R values in BS and DS are qualitatively similar to the analogous quantities in Si(111). However the structure of the minima is perceptibly more complex on Si(100) than on Si(111). In fact at the site m_0 in DS Ag is preferentially absorbed at z=0. However the x, y dependence of E_b is a fairly flat basin and the adsorption site expands about 0.3 Å along both directions. At m'_0 and m_1 the two minima extend from z=0 to ∼1.5 Å above the surface. Furthermore, as shown by the R values, adsorption in these two sites generates noticeable elastic effects, which are absent from m_0. In this location the total dipole component is of one order of magnitude lower than in m'_0 and m_1 and this indicates a more even charge distribution than in the other two cases.

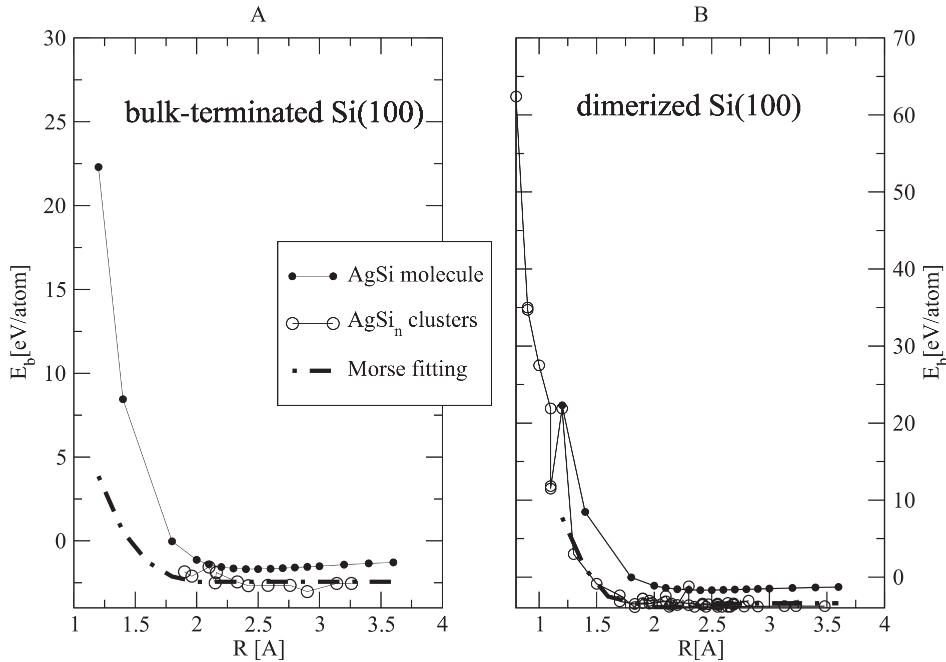

Fig. 3. Plot of the binding energy E_b for the bulk-terminated (A) and the dimerized (B) Si(100) surface.

These properties, at variance with the ones of Ag/Si(111), are attributed to the different structure and orientation of the dangling silicon orbitals on the two surfaces and the consequence is that the strength of binding increases from about 3 eV/Ag atom to 4.0 eV/Ag atom in passing from Si(111) to DS.

Second, the difference between the bulk-terminated and the dimerized Si(100) is perceptible and appears on both the values of E_b and on the locations of the minima. These divergences should clearly appear in experiments and should help clarify the structure of the deposited surface. On this point a short comparison with literature results is in order. The DeFT values of binding are supported by the optical and X-ray experiments reported above [11,17]. However from STM and RBS observations [9,14] the adsorption site on DS is identified with a cave site between two dimer rows at an height z about 0.05 Å above the surface. This site, indicated as m_e in Figure 1b, is slightly displaced from m_0. In DeFT calculations m_e shares the x, y expansion of m_0 and its E_b values are of about 0.4 eV above it. The calculations in [19] show several features consistent with DeFT, i.e. adsorption occurs always in a hollow site and the energy differences among possible sites are in range of a few tenths of eV. These calculations favor a site of the type m_e which however, in contradiction with experiments, lies at 1.12 Å above the surface. As shown by the literature on Ag/Si(111), adsorption calculations critically depends on the formulation of the Hamiltonians and of the electronic charge. This accounts for the differences between [19] and DeFT whereas experiments [9] show only that Ag is in the trench between the dimer rows and the m_e locations is obtained just by suggestion.

Third, according to early calculations on Ag/Si(111), the features of the adsorbed system can be represented, at least to a first order approximation, by the Ag-Si molecule, whose E_b vs. R is also shown in Fig. 3). In DeFT calculations the optimal bond length and binding energy of Ag-Si are 2.5 Å and −3.2 eV/atom, respectively. These values can be justified by averaging between the bond energy and the bond length of crystalline Silicon and of the Ag-Ag molecule (i.e. 2.35 Å and 4.63 eV for Silicon and 2.48 Å and 0.83 eV/atom for Ag-Ag, respectively). In Ag-Si the charge exchanged between the two atoms is approximately 0.15 and derives from the sp_3 charge of Si and the s, p and d charges of Ag. The value 0.15 is also representative of the charge exchanges observed in Ag/Si(100) (similar data are reported in [2,7]) and also the R and E_b values are close in the two cases. In the context of this work the important aspect of these similarities is that the interaction of Ag with the silicon surface can be viewed as a sum of pair-wise molecular interactions and can therefore be represented with a simple two-body potential. For MD calculations the E_b vs. R of Si(100) has been fitted with a Morse potential (also adopted in [19]) of the form

$$V(R) = D(\exp(-\alpha_1(R-R_o)) - \gamma \exp(-\alpha_2(R-R_o))). \quad (1)$$

The value of α_1,α_2, R_o and γ is 1.8 [Å^{-1}],1.4 [Å^{-1}], 3.2 [Å] and 2.2 for both DS and BS. The value of D is 1.0 eV and 0.8 eV for DS and BS, respectively.

The plots of $V(R)$ in Figure 3 clearly show the excellent fitting obtained with this simple potential. It is added that at the distances of maximum binding, i.e. for R between 2 and 3.5 Å, the difference between E_b and $V(R)$ is approximately 7% for both BS and DS.

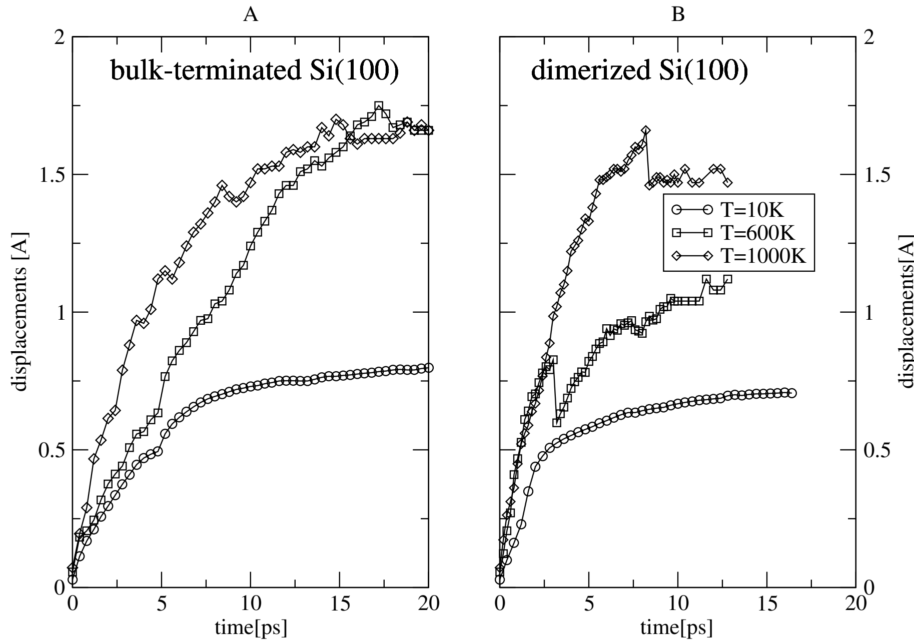

Fig. 4. Displacements of Ag atoms deposited on the bulk-terminated (A) and on the dimerized Si(100) surface (B) at a variable deposition temperature.

4 The motions of the deposited adatoms

Under experimental conditions Ag films are deposited at a temperature T in the range from 300 to 1000 K. These high temperatures stimulate atomic motions and generate displacements of the deposited atoms. It is therefore important to understand the effects of this dynamics on the final adsorption locations and the MD calculations were developed with this purpose. These calculations were started with the Ag incidence points distributed along the line containing d_0 on BS and m_0 and m_0' on DS (Fig. 1b). The other incidence conditions were: a spacing of approximately 1 Å along x with y variable from -1.5 Å to 1.5 Å and a height z=0.2–0.5 Å above the surface.

In Andersen dynamics the average temperature T of the system is kept constant by fictitious collisions which act as a thermal bath. However the temperature of some parts of the system may differ from the average one and this leads to a dynamical evolution of the velocities and coordinates of the atoms forming the system. Accordingly, in a MD run the Ag atoms are deposited on the substrate, which is thermostated at T by the thermal bath, with a temperature corresponding to their kinetic energy E. This leads to a temperature gradient with maximum near the surface. The following transient is dictated by the achievement of T in both the adsorbate and in the silicon surface.

The evolution in time of the motions of the deposited Ag atoms is shown in Figures 4, 5 and 6. Figure 4 illustrates the displacements $\langle d \rangle$ of these atoms on Si(100) for either the bulk-terminated or the dimerized surface in a temperature range from 10 K to 1000 K. Figures 5 and 6 show the z, x, y components of $\langle d^2 \rangle$ for the two surfaces.

On both BS and DS the displacements consist of a sharp rise followed by a flat asymptote attained in a time of approximately 5–10 ps (Fig. 4). Furthermore, the presence of metastable states is revealed by the fact that the deposited atom maintains for some time the same characteristics of motions. These states however collapse by a violent scattering event which alters the motion and leads to a sudden jump in the d curves. The final asymptote is important. It shows that an equilibrium adatom configuration is dynamically achieved and can be compared with the stationary configurations illustrated in the previous section. The corresponding values of $\langle d \rangle$ are well above the amplitude of thermal lattice excitations but smaller than a thermal jump length (according to the interatomic distances on the silicon surface this distance varies from 2.3 to 3.8 Å). At low temperatures the displacements arise from motions along z (Figs. 5 and 6) and are directed away from the silicon surface. The increase of T has a different effect on the two surfaces. On BS longer displacements with large transversal x, y components are observed at high T while on DS only the increase of the z component is produced (Figs. 4, 5 and 6). The effect is attributed to the large distance between dimer rows, 5.33 Å in DS, in comparison with 3.83 Å in BS. This large distance limits the transversal interactions and this, in turn, reduces the corresponding motions.

The z-directed displacement is a predominant feature of the motions of the deposited atoms and is independent on the incidence conditions. This was proved by a large number of calculations performed with a kinetic energy E of the deposited Ag in the range from 0.01 to 0.1 eV with grazing and normal incidence or with an incidence isotropically distributed among x, y and z. The motions along z have therefore to be regarded as a property of the Ag-Si interactions and of the lattice structure and their existence represents a central difference with

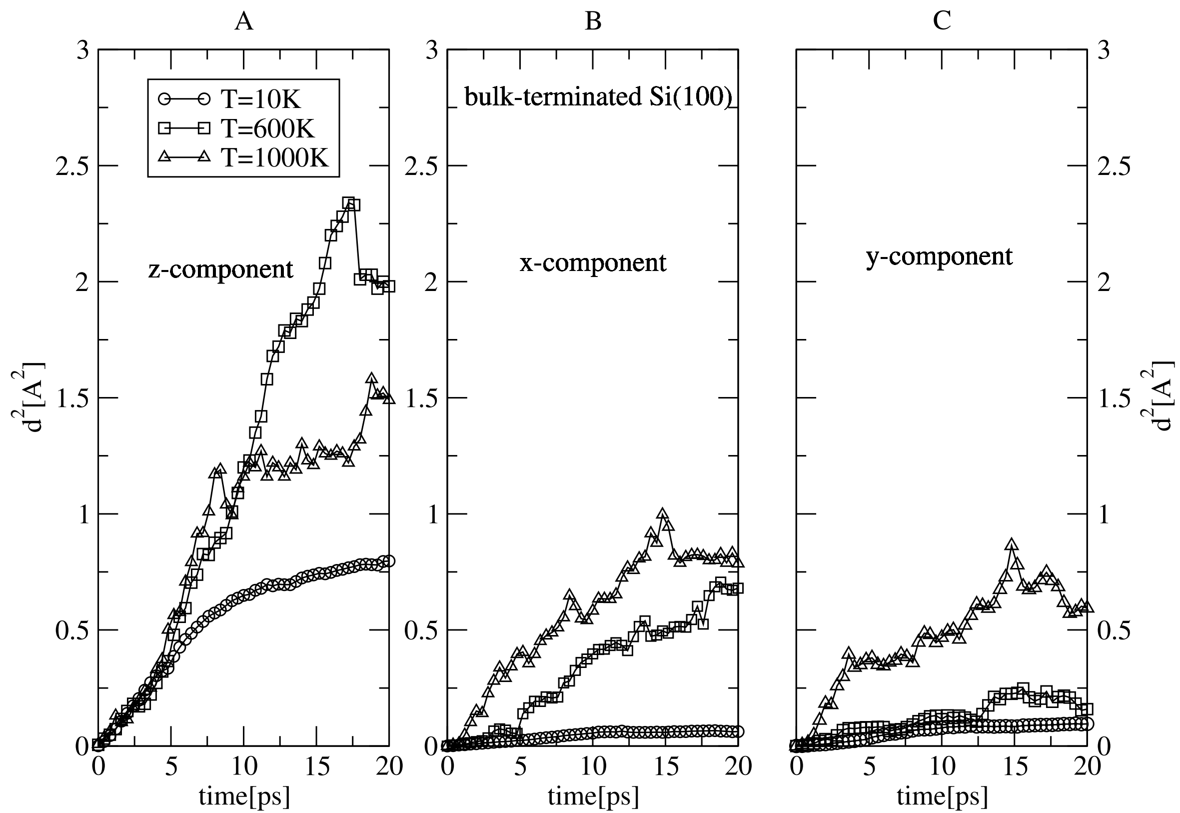

Fig. 5. z, x, y components of the square displacements of deposited Ag atoms on the bulk-terminated Si(100) surface.

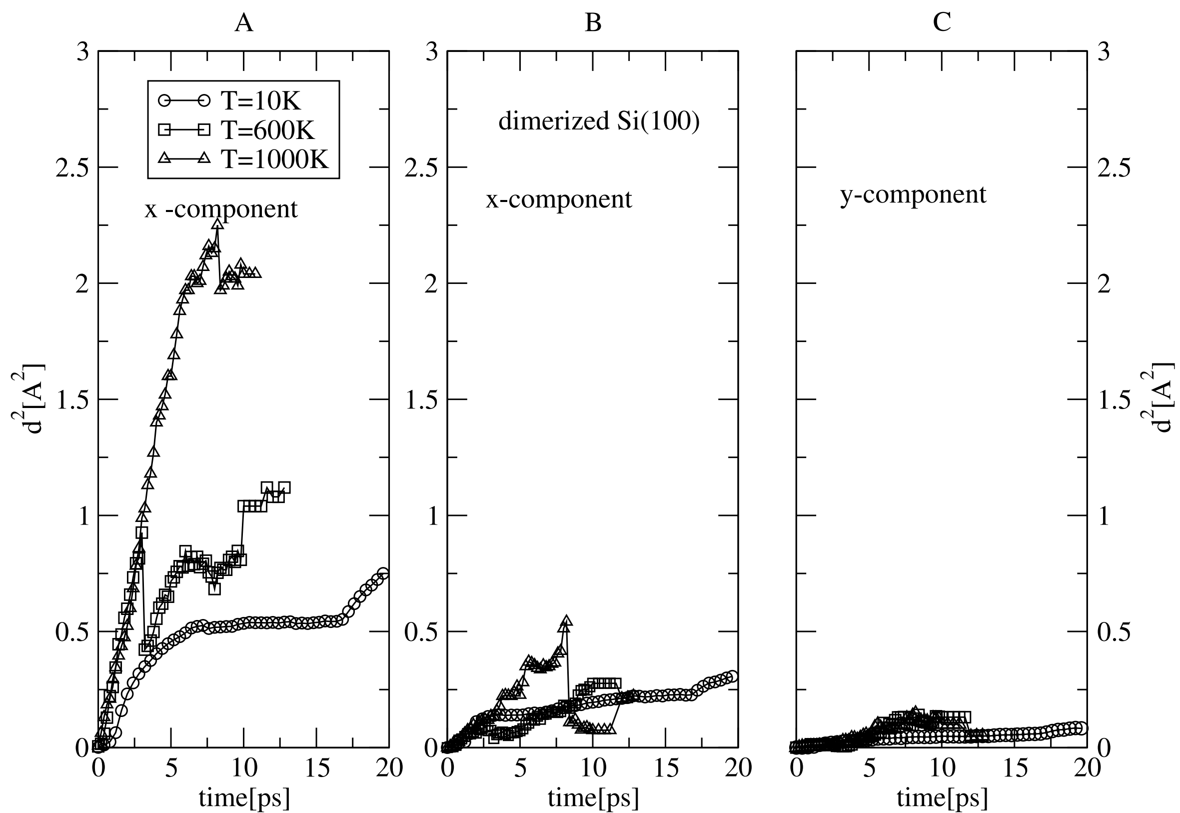

Fig. 6. z, x, y components of the square displacements of deposited Ag atoms on the dimerized Si(100) surface.

respect to other systems where motions driven parallel to the surface have been observed [25]. Also the stationary study of diffusion barriers in [19] shows only anisotropic motions in the x, y plane. At variance with these results, the displacements obtained from MD have to be viewed as a 'reverse' channeling due to a prevailing z-force component directed above the surface instead that under it. In fact, Ag atoms moving in the trench between surface atoms experience nearly equal y-forces arising from the two facing rows. These forces have an opposite direction and cancel each other. Also the x-force component is small due to the balance of the action of the silicon atoms in front of the diffusing Ag and on its rear. Therefore only a net force along z arises from the the different heights of the deposited atom and of the silicon lattice. At large distance this force is attractive, as shown by the binding minimum of E_b (Fig. 3). However, when Ag approaches the silicon lattice, the force changes from attractive to repulsive at small R. This pushes Ag above the surface and is the source of the z-directed displacements.

To analyze the stability of the adsorption sites described in the previous paragraph a close study was performed on trajectories of atoms deposited on DS along the lines containing m_0 and m'_0 (Fig. 1b). It was found that, due to the high symmetry of these locations, the forces are small and the atoms have limited motions. In fact, their displacements are from one-half to one-third smaller than the ones in Figure 4 which have been obtained by averaging on incidence points distributed along the two lines with a variable y. Therefore atoms adsorbed at m_0 and m'_0 at low temperature are lifted above the surface and the total displacement, upward and sideways, amounts to some tenths of Å. In this way the stability of these adsorption sites is maintained also under dynamical conditions. However it is plausible that the combined effect of these displacements and other factors not accounted for in the simulations (notably Ag-Ag interactions) lead to the attainment of the m_e site suggested by the experiments.

As a final remark it is added that a complex dynamics was observed for surface and near-surface silicon atoms. Prior to deposition the disorder of these atoms arises from thermal excitation and is dictated by the value of T. The interaction with the deposited Ag causes displacements and lattice relaxation with the mode illustrated by Figure 2. This effect leads also to a further displacement of the deposited Ag. The progressive equilibration of the system quenches the motions of silicon atoms and reduces the disorder. This evolution suggests that the deposited surface, without changing its essential morphology, may considerably differ from the one in the absence of deposition.

5 Conclusions

In conclusion, DeFT calculations show that the properties of adsorption on Ag/Si(100) are perceptibly different from the ones of Ag/Si(111) and the preferred adsorption sites have a remarkable dependence on the structure of the exposed surface. Molecular dynamics calculations indicate that the dynamics of the atomic motions may lead to large displacements, unless the deposited atoms fall directly into the privileged adsorption sites.

In the section above a comparison with literature results has been made. Here is only added that both DeFT and MD calculations have been conducted in the dilute limit at low coverage. This does not allow to make predictions on the structure of the growing films. However the propensity of the deposited atoms to occupy hollow sites between atomic rows, observed in DeFT calculations, suggests the formation of linear chains without intermixing with the silicon surface. This picture is also supported by MD calculations which show z motions directed away from the surface with limited lateral displacements. These features are in agreement with the linear chains observed by STM at submonolayer coverage [9,11].

This study has been sponsered by MIUR under contract FIRB101M9Tl.

References

1. V. Barone, G. del Re, G. Lelay, R. Kern, Surf. Sci. **99**, 223 (1980)
2. A. Julg, A. Allouche, Int. J. Quantum Chem. **XXII**, 739 (1982)
3. G. Lelay, Surf. Sci. **132**, 169 (1983)
4. A. Fortunelli, O. Salvetti, G. Villani, Surf. Sci. **244**, 344 (1991)
5. S.H. Chou, A.J. Freeman, S. Grigoras, T.M. Gentle, B. Delley, E. Wimmer, J. Chem. Phys. **89**, 5177 (1988)
6. C.T. Chan, K.M. Ho, Surf. Sci. **217**, 403 (1989)
7. H. Aizawa, M. Tsukada, Phys. Rev. B **59**, 10923 (1999)
8. M. Hanbucken, M. Futamoto, J.E. Venables, Surf. Sci. **147**, 433 (1984)
9. A. Samsavar, E.S. Hirschorn, F.M. Leibsle, C.T. Chiang, Phys. Rev. Lett. **63**, 2830 (1989)
10. K. Nishimori, H. Tokutaka, T. Tamon, S. Kishida, N. Ishihara, Surf. Sci. **242**, 157 (1991)
11. Y. Borensztein, R. Alameh, Appl. Surf. Sci. **65-66**, 735 (1993)
12. T. Michely, M.C. Reuter, M. Copel, R.M. Tromp, Phys. Rev. Lett. **73**, 2095 (1994)
13. D. Winau, H. Itoh, A.K. Schmid, T. Ichinokawa, Surf. Sci. **303**, 139 (1994)
14. K. Kimura, O. Kazuomi, M. Mannami, Phys. Rev. B **52**, 5737 (1995)
15. S.H. Shivaprasad et al., Surf. Sci. Lett. **344**, l1245 (1995)
16. H.W. Yeom, I. Matsuda, K. Tono, T. Ohta, Phys. Rev. B **57**, 3949 (1998)
17. I. Matsuda, H.W. Yeom, K. Tono, T. Ohta, Phys. Rev. B **59**, l5784 (1999)
18. O. Takeuci, M. Kageshima, H. Sakama, A. Kawazu, Jpn J. Appl. Phys. **40**, 4414 (2001)
19. R.H. Zhou, P.L. Cao, L.Q. Lee, Surf. Sci. Lett. **290**, L649 (1993)
20. A. St-Amant, W.D. Cornell, T.A. Halgren, P.A. Kollman, J. Comp. Chem. **16**, 1483 (1995)
21. A.M. Mazzone, Phil. Mag. B **77**, 1011 (1998)
22. A.M. Mazzone, Appl. Phys. A **63**, 217 (1996)
23. D.J. Oh, R.A. Johnson, J. Mat. Res. **3**, 471 (1988)
24. J. Tersoff, Phys. Rev. Lett. **56**, 632 (1986)
25. S. van Dijken, L.C. Jorritsma, B. Poelsema, Phys. Rev. B **61**, 14047 (2000)